Acceleron Aerospace Journal || AAJ.11.2106-2508
Volume 4, Issue 2, pp (886-910)
Project Paper
E-ISSN- 2583-9942 || DOI: 10.61359/11.2106-2508

From Earth Escape to Lunar Touchdown: A Simulated Lunar Lander Mission

Syleen Edwards *, Sunny Kabrawala

Spaceflight Mechanics Intern, Space Technology and Aeronautical Rocketry, and Embry-Riddle Aeronautical University, 1 Aerospace Blvd., Daytona Beach, FL, USA, 32114

Abstract: This report investigates the application of design thinking principles to optimize the trajectory and operations of a lunar lander. By considering the spacecraft as the "user" within the design thinking framework, we aim to identify and address critical challenges during key mission phases: Earth Escape, Orbital Insertion, Lunar Transfer Trajectory Injection, and Powered Descent & Lunar Landing. Leveraging the General Mission Analysis Tool (GMAT), we translate design thinking solutions into testable virtual prototypes, allowing for iterative refinement and optimization of the mission plan. This approach prioritizes efficiency and functionality, ultimately paving the way for more cost-effective and successful lunar exploration endeavors.

Table of Contents

1. Introduction

Landing a spacecraft on the Moon is a remarkable demonstration of human ingenuity and engineering prowess. While it might seem straightforward, the journey from Earth to lunar touchdown requires meticulously planned maneuvers, precise calculations, and skillful execution. This report explores how design thinking, a structured approach to innovation, can be applied to optimize the trajectory and operations of a lunar lander.

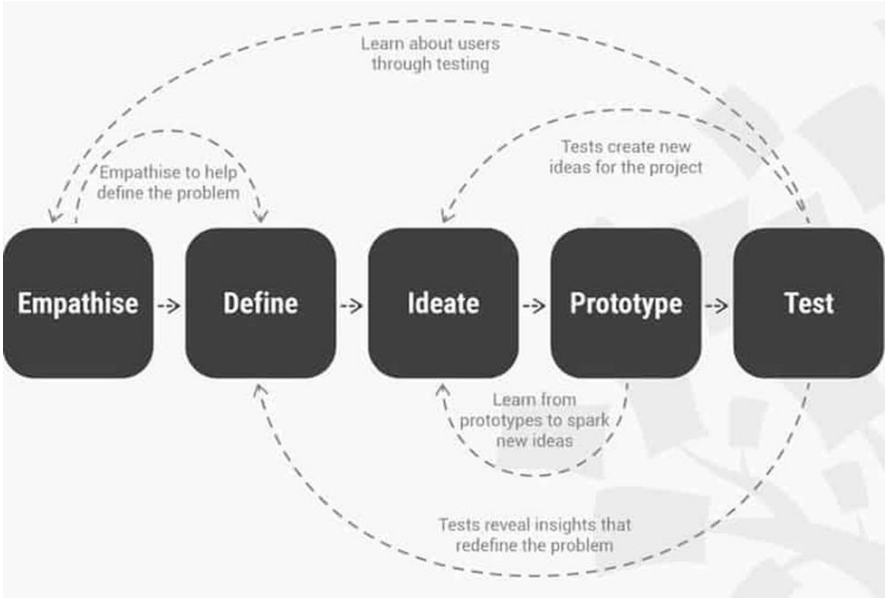

Figure-1 Design Thinking Framework (Greer, 2020)

As depicted in Figure 1, the design thinking framework provides a structured approach to innovation by focusing on the user's needs. In this context, the spacecraft itself is the "user." By leveraging this framework, our goal is to utilize our understanding of the spacecraft's technical, operational, and environmental requirements to

*Spaceflight Mechanics Intern, Space Technology and Aeronautical Rocketry, and Embry-Riddle Aeronautical University, Aerospace Blvd., Daytona Beach, FL, USA, 32114. **Contact: edwardssyleen@gmail.com.**
** Received: 15-February-2025 || Revised: 28-February-2025 || Accepted: 28-February-2025 || Published Online: 28-February-2025.

identify challenges it will encounter during each mission phase: Earth Escape, Orbital Insertion, Lunar Transfer Trajectory Injection, and Powered Descent & Lunar Landing. By acknowledging these challenges, we can prioritize specific operational hurdles and develop diverse solutions for various mission aspects, particularly those related to orbital mechanics. We will use GMAT to translate our design thinking solutions into a testable format. This powerful software is designed specifically for simulating spacecraft trajectories and enables us to create a virtual prototype for the critical phases of the lunar descent mission. This comprehensive virtual testing allows us to assess and refine our design before finalization. This iterative approach promises a more nuanced perspective on lunar lander design, prioritizing efficiency and functionality. By following the design thinking framework, this report aims to develop a mission plan that optimizes the spacecraft's journey and paves the way for future, cost-effective lunar exploration endeavors.

2. Background

This section outlines the fundamental scientific and design principles that underpin a successful lunar lander mission. These principles can be broadly categorized into two main areas: rocket stability and orbital mechanics.

2.1 Rocket Stability

Rocket stability is a fundamental principle for a successful lunar landing mission. Newton's Second Law provides the foundation for understanding the forces acting on a rocket during flight, while the rocket equation and kinematic motion allows us to analyze how to achieve and interpret the resulting motion and trajectory. This understanding will enable engineers to optimize factors like nose cone design to enhance aerodynamic performance. Strategic alignment of the center of mass and center of pressure is also crucial for maintaining stability. These factors, alongside proper control systems, ensure controlled ascent and accurate trajectory, which is essential for any space mission.

2.1.1 Newton's Second Law

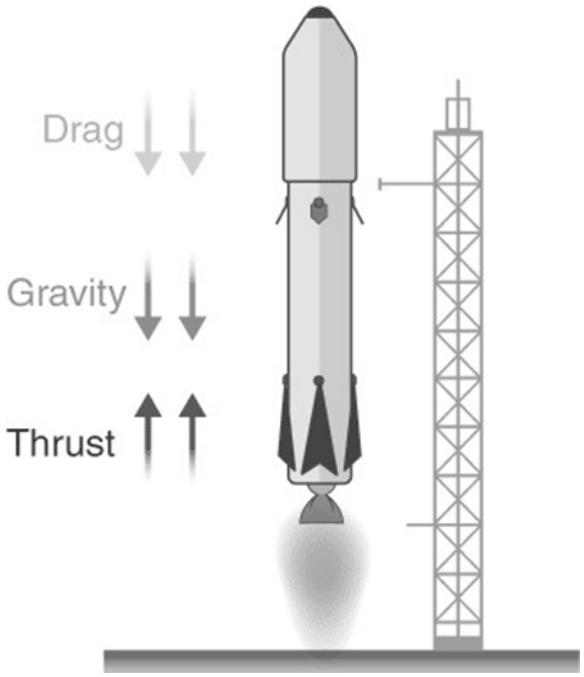

Figure-2 Rocket Propulsion Diagram (Byjus, n.d.)

Our journey into space flight begins with the fundamental exploration of motion itself. Specifically, Newton's Second Law of Motion:

$$F = m * a \tag{1}$$

Equation (1) provides the "why" of motion, serving as the foundation for understanding the forces that govern rocket propulsion. This law states that the net force (F) acting on an object is equal to its mass (m) multiplied by its acceleration (a). In simpler terms, the force acting on an object determines how much that object speeds up or

slows down. $F = m * a$ is crucial for understanding and achieving rocket stability. It allows us to understand and predict how various forces acting on the rocket – thrust, gravity, and drag (the aerodynamic force opposing the rocket's motion through the air, as depicted in Figure 2) – influence its movement and ultimately, its ability to maintain a desired trajectory.

To maintain a desired trajectory, thrust—the primary forward-acting force generated by expelling propellant through the rocket engines—must overcome all opposing forces, particularly weight and drag, during the critical ascent phase. If thrust fails to exceed these opposing forces, the rocket may experience reduced acceleration, increased aerodynamic heating, deviations from the planned trajectory, or even failure to reach orbit. To mitigate these risks, engineers prioritize optimizing both the thrust-to-weight and thrust-to-drag ratios in rocket design and mission planning.

2.1.2 The Tsiolkovsky (Rocket) Equation

Building on the concept of thrust as the driving force behind rocket motion, we turn to the Tsiolkovsky Rocket Equation—a cornerstone of rocketry that expands on Newton's Second Law. Newton's law establishes that a force acting on a mass produces acceleration, and in rocketry, this force is generated by expelling propellant. As fuel is consumed during flight, the rocket's mass decreases, resulting in increased acceleration for a constant level of thrust. This dynamic interplay is important for understanding how rockets achieve the velocities needed for space travel. The Tsiolkovsky Rocket Equation mathematically expresses this relationship as:

$$\Delta v = v_e ln(m_0/m_f) \tag{2}$$

where:

- Δv represents the total velocity change that the rocket achieves. It is the key value used to calculate how much Δv is needed to complete specific maneuvers.
- V_e is the speed at which the exhaust gases leave the rocket's propulsion system (measured relative to the rocket). As displayed in the following equation, it depends on the specific impulse (Isp) of the engine and the gravitational constant. Higher exhaust velocity allows for more efficient use of fuel, providing a greater change in velocity for a given amount of propellant.

$$V_e = I_{sp} * g_0 \tag{3}$$

- I_{sp} is the specific impulse of the rocket's engine (a measure of how efficiently the rocket uses fuel).
- g_0 is the standard gravitational acceleration on Earth (9.81 m/s2).
- m_0 is the initial mass of the spacecraft, including fuel.
- m_f is the final mass of the spacecraft after fuel has been expended.

This equation is essential for calculating how much Δv is available for maneuvers, determining how much of the rocket's initial mass must be allocated to fuel, and assessing how efficiently that fuel is used.

The rocket equation also directly impacts the thrust-to-weight ratio, a critical parameter for rocket performance. As the rocket's mass decreases with fuel consumption, the thrust-to-weight ratio improves, allowing the vehicle to accelerate more effectively. This improvement is especially crucial during the ascent phase, where sufficient thrust must overcome gravity and drag. A higher thrust-to-weight ratio not only ensures better acceleration but also reduces the time the rocket spends in high-drag regions of the atmosphere, thereby improving overall efficiency.

By providing a framework for understanding the relationship between mass, thrust, and velocity, the rocket equation informs key design decisions, such as optimizing fuel usage, selecting engine specifications, and balancing payload capacity. These factors are fundamental to achieving the desired trajectory and ensuring the rocket's ability to overcome the opposing forces discussed earlier.

2.1.3 Kinematic Motion

While Newton's Second Law provides the fundamental "why" of motion, and the rocket equation quantifies the "how" of changing that motion through propellant expulsion, a complete understanding of a rocket's trajectory requires a multi-disciplinary approach.

As discussed previously, the Tsiolkovsky Rocket Equation is a cornerstone. It relates the change in velocity of a rocket to its initial mass, final mass, and exhaust velocity. By optimizing the parameters in this equation, engineers can design rockets that achieve the necessary Δv for various space missions. However, the equation doesn't directly address how the rocket moves under the influence of forces.

This is where kinematic motion equations come in. They describe the motion of an object experiencing constant acceleration, like a rocket during its powered ascent phase. These equations, like:

$$v = v_0 + at \ (final\ velocity = initial\ velocity + acceleration \times time \quad (4)$$

$$\Delta x = ½(v_0 + v)t \ (displacement = average\ velocity \times time) \quad (5)$$

$$\Delta x = v_0 t + ½at^2 \ (displacement = initial\ velocity \times time + ½ \times acceleration \times time^2) \quad (6)$$

$$v^2 = {v_0}^2 + 2a\Delta x \ (final\ velocity2 = initial\ velocity2 + 2 \times acceleration \times displacement) \quad (7)$$

allow us to analyze how the thrust-to-weight ratio impacts a rocket's trajectory and ascent profile. For instance, a higher T/W ratio translates to greater acceleration (a) in the kinematic equations. This higher acceleration results in a faster increase in velocity (v) and a steeper ascent profile (Δx) during powered flight.

Calculating the rocket's position and velocity at different times based on its acceleration (derived from T/W) gives us valuable insights into its behavior. This information is crucial for optimizing the rocket's design and trajectory to achieve the desired flight path.

2.1.4 Nose Cone Optimization

In terms of achieving an optimal thrust-to-drag ratio during launch, one strategy is to streamline the vehicle's shape, particularly the nose cone, where air pressure is highest. This is because drag is directly affected by the surface area of the vehicle in contact with the air. The drag equation

$$Drag = ½\ density * reference\ area * drag\ coefficient * velocity^2 \quad (8)$$

highlights this relationship, where the reference area is often the cross-sectional area of the nose cone.

However, drag is not solely dependent on surface area. It also increases significantly with the velocity of the vehicle relative to the air. Therefore, the challenge lies in balancing these two factors.

The shape of the nose cone, in conjunction with the vehicle's velocity, plays a crucial role in the formation of shockwaves as the vehicle reaches hypersonic speeds. Together, these factors dictate whether the shockwave remains attached or becomes detached, impacting aerodynamic heating, drag (as described by the equation), and overall vehicle stability.

Figure-3 Oblique Shock (Ansys Innovation Courses, n.d.)

Due to their geometry, sharp nose cones experience an attached shockwave, meaning the shockwave attaches directly to the tip of the nose cone (Figure 3). While this form of shock offers the benefit of presenting a smaller profile to the oncoming air, potentially reducing drag at lower speeds, at hypersonic speeds, the air cannot smoothly follow the sharp point. This leads to flow separation—the inability of the airflow to stay attached to the cone surface. The consequences of flow separation include a more turbulent wake, increased drag, and increased heating.

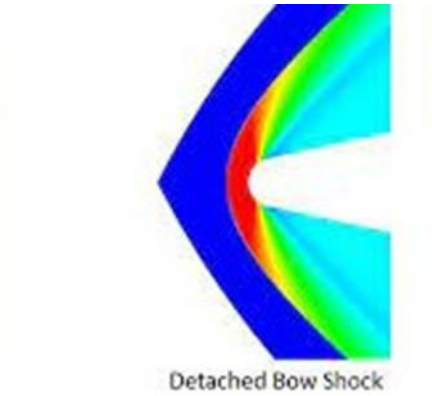

Figure-4 Detached Bow Shock (Ansys Innovation Courses, n.d.)

On the other hand, spherically blunt nose cones experience a detached shockwave, also known as a bow shock. As depicted in Figure 4, bow shocks are located further ahead of the cone. This detached bow shock formation, in comparison to sharp cones, allows for a more gradual deflection of airflow, which translates to lower drag on the launch vehicle. This reduction in drag can help maintain higher velocities during the critical phases of flight. Additionally, while a bow shock still creates a region of high pressure and temperature, the larger surface area of a blunt nose cone helps distribute the heating more evenly, reducing the peak intensity at the stagnation point.

In summary, while sharp nose cones might offer a slight advantage in drag at very low speeds, their limitations at hypersonic speeds make them unsuitable for launch vehicles. Despite having a larger frontal area, spherically blunt nose cones offer significant advantages in managing drag, and thermal loads, and maintaining stable airflow during the critical launch phase. This is why more than 99% of launch vehicles are designed with these types of nose cones.

2.1.5 Centering Forces

The thrust-to-drag ratio is also dependent on the relationship between the vehicle's center of pressure (CoP) and center of mass (CoM).

A rocket's CoM is the point where its mass is balanced, representing the average location of its overall mass distribution, including components such as the payload, fuel, and structural elements. This dynamic point shifts during flight as fuel is consumed, affecting the rocket's stability and control1. The CoM also serves as the point around which the rocket naturally rotates if subjected to external forces, making its position critical for maintaining a stable trajectory1.

The CoP is a theoretical point representing the average location of aerodynamic forces, such as drag, which arise from the interaction between the rocket's surface and the surrounding airflow. It is referred to as a theoretical point because aerodynamic forces are not uniformly distributed across the rocket's surface1. For example, as discussed earlier, the nose cone, which directly faces the airflow, experiences high pressure, while this pressure diminishes along the rocket's body.

The CoP's position relative to the CoM plays a vital role in determining the rocket's stability during flight, as it influences how the rocket responds to aerodynamic forces and external disturbances. Understanding and managing the CoP and CoM are essential for ensuring a controlled and stable ascent.

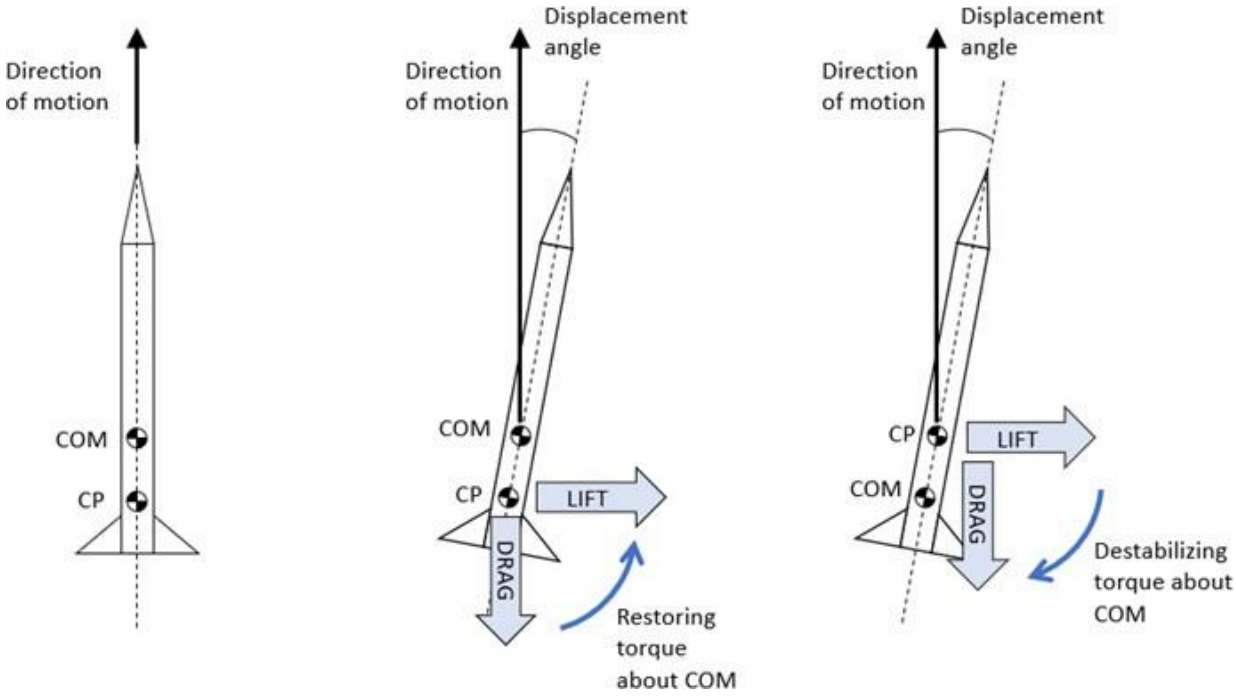

Figure-5 Centering Forces (Finio, 2023)

As displayed in Figure 5, for a rocket to be stable, the CoP must be positioned behind the CoM along the flight path. This alignment ensures that any aerodynamic forces will produce a restoring moment that returns the rocket to its intended orientation if it deviates from its flight path. Conversely, if the CoP is in front of the CoM, disturbances created by aerodynamic forces will create a torque that amplifies any deviations, leading to instability.

To ensure the CoP is correctly positioned relative to the CoM, engineers often add fins or other aerodynamic surfaces to the lower part of the rocket to move the CoP rearward. Additionally, they adjust the shape of the rocket and strategically place components such as fuel tanks, engines, and payloads within the rocket.

In conclusion, in conjunction with optimizing the nose cone design, understanding the rocket's center of gravity, and centering forces, kinematic modeling plays a crucial role in achieving a stable flight path. By carefully balancing the aerodynamic forces acting on the vehicle, we can ensure that the flight remains stable and controlled, even at high speeds

2.1.6 Exercise 1: Rocket Trajectory Prediction and Stability Analysis

With a fully optimized and stable vehicle, we can now proceed to the critical task of calculating its launch trajectory. By considering factors such as the vehicle's mass, gravitational constant, thrust, nose cone diameter (to determine drag), drag coefficient, and air density, we can compute essential trajectory parameters at various stages of the ascent process. These include:

- Initial Velocity: Essential for overcoming gravity and reaching the target orbit.
- Altitude: Determines atmospheric drag and gravitational forces.
- Drag Force: Opposes the rocket's motion, increasing with velocity and altitude.
- Gravitational Force: Pulls the rocket towards Earth.
- Net Force: The combined effect of thrust, drag, and gravity.
- Acceleration: The rate of change of velocity.
- Net Velocity: The overall speed and direction of the rocket.

Understanding these parameters is crucial for making timely adjustments to the trajectory, navigation, and mission objectives, optimizing fuel usage and performance, and enabling precise targeting for orbital maneuvers, planetary landings, or scientific observations, ensuring mission goals are met effectively.

Consider the following example: For a launch vehicle with a mass of 10 kg, a thrust of 1000 Newtons, a nose cone diameter of 0.1 meters, a drag coefficient of 0.45, and an air density of 1.225 kg/m³, we can calculate these trajectory parameters to determine its performance and success in achieving orbit.

Parameters	
Mass	10
Thrust	1000
g-Constant	9.8
Diameter	0.1
Area	0.00785
Cd	0.45
Density	1.22

Trajectory Parameters							
Time	Initial V	Altitude	D	Mg	Fnet	a net	v net
0.1	0	0	0	98	902	90.2	9.02
1	9.02	4.059	0.175317	98	901.8247	90.18247	81.16422
2	90.18422	53.66111	17.52561	98	884.4744	88.44744	88.44744
3	178.6317	188.0691	68.75889	98	833.2411	83.32411	83.32411
4	261.9558	408.3628	147.8659	98	754.1341	75.41341	75.41341
5	337.3692	708.0252	245.2578	98	656.7422	65.67422	65.67422

Figure-6 Calculating Trajectory Parameters

Initial Calculations:

1. **Initial State:** At t=0.1 seconds, the rocket is stationary with zero initial velocity, altitude, and drag.
2. **Weight Force:** Calculate the constant weight force acting on the rocket by multiplying its mass by the Earth's acceleration.

$$F_w = m * 9.81 m/s2 \tag{9}$$

3. **Net Force:** Determine the net force acting on the rocket at each time step using the equation:

$$Net\ Force\ =\ Thrust\ Force\ -\ Weight\ Force\ -\ Drag\ Force \tag{10}$$

4. **Net Acceleration:** Calculate the acceleration using Newton's Second Law (Equation (1)).
5. **Net Velocity:** Determine the net velocity by multiplying the net acceleration by the time interval.

$$V_{net}\ =\ A_{net} * t \tag{11}$$

Iterative Calculations:

Having solved data at t = 0.1 seconds, we now have a solid foundation for our launch simulation. For the remaining time intervals (t = 1-5 seconds), we will follow a structured iterative approach:

1. Initial Velocity: Use the final velocity from the previous time step as the initial velocity for the current time step.
2. Calculate Altitude: Determine the altitude using the average velocity over the time interval:

$$Altitude\ =\ ((V_0\ +\ V_{net})\ /\ 2)\ *\ (t - t_0). \tag{12}$$

3. Calculate Drag Force: Compute the drag force based on the initial velocity, air density, reference area, and drag coefficient (Equation (9)).
4. Calculate Net Force: Subtract the weight and drag forces from the thrust force to determine the net force acting on the rocket (Equation (10)).
5. Calculate Net Acceleration: Use Newton's Second Law (Equation (1)) to find the acceleration resulting from the net force.
6. Update Velocity: Calculate the net velocity for the current time step by multiplying the net acceleration by the time interval by the initial velocity (Equation (11)).

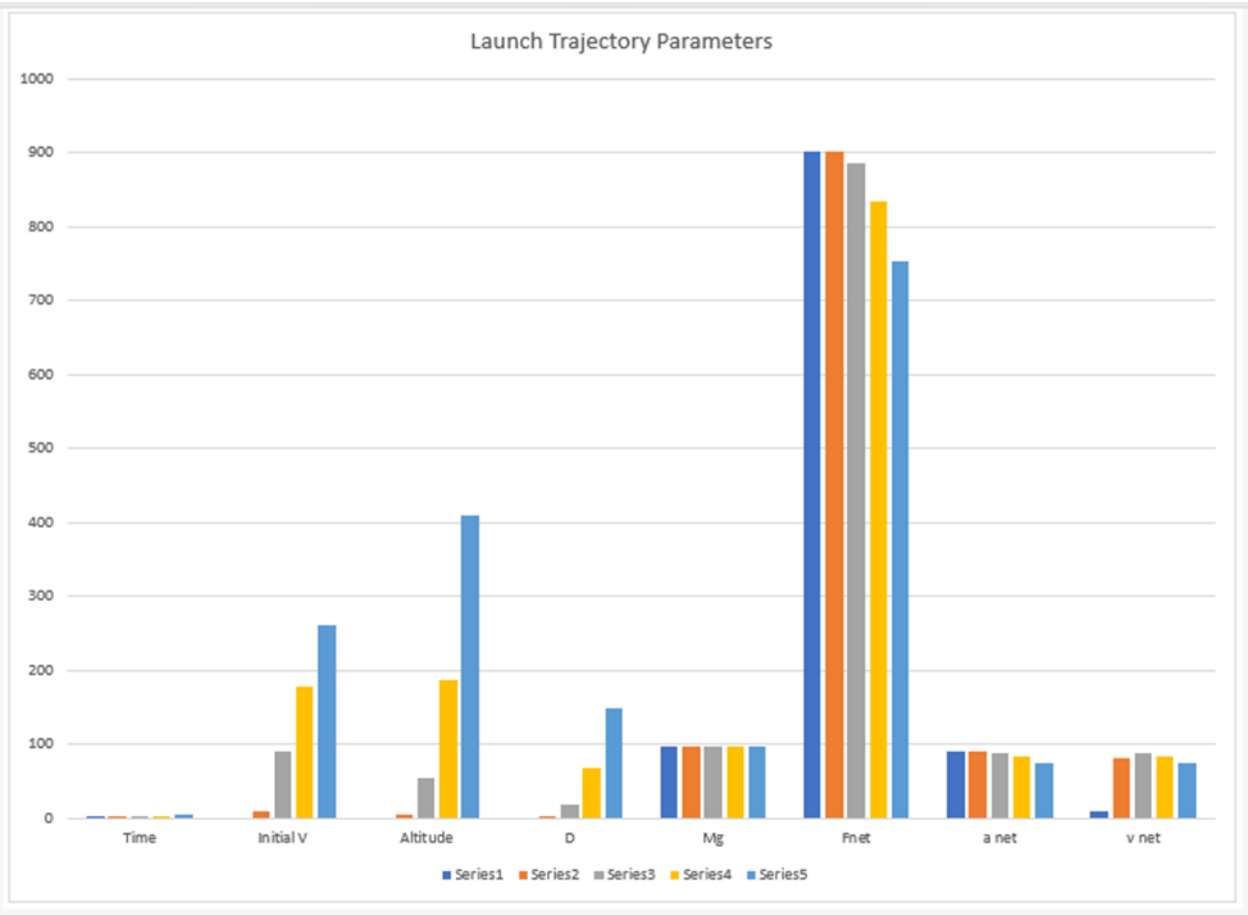

Figure-7 Data Interpretation

The graph above illustrates the calculated trajectory of the rocket during the first seconds of its ascent. At t=5s and an altitude of 708.02 m, air resistance is significant and increases with velocity, requiring the rocket to generate sufficient thrust to overcome drag and gravity. As fuel is consumed, the rocket's mass decreases, which would typically lead to increased acceleration. However, during this phase, acceleration might decrease due to the rapidly increasing drag force, which grows quadratically with velocity in the dense lower atmosphere. Additionally, if the thrust remains constant while the opposing forces (drag and gravity) increase faster than the reduction in mass, the net force acting on the rocket decreases. This, coupled with potential engine throttling to manage structural stress, could lead to a temporary reduction in acceleration despite the reduction in mass.

As Time Progresses:

- **Initial Velocity:** The rocket's velocity increases steadily as thrust overcomes drag and gravity.
- **Altitude:** The altitude increases at an accelerating rate as the rocket climbs higher, eventually moving into thinner atmospheric layers where drag decreases.
- **Drag:** As the rocket gains altitude and enters regions of lower air density, the drag force begins to decrease despite increasing velocity.
- **Net Force:** As drag diminishes at higher altitudes and the rocket's mass decreases, the net force increases, allowing for greater acceleration.
- **Net Acceleration:** Net acceleration begins to increase as the rocket burns fuel, reducing its mass, and as drag lessens with altitude.
- **Net Velocity:** The velocity increases steadily over time, accelerating faster as drag decreases and a larger proportion of thrust contributes to forward motion. By the time the rocket exits the lower atmosphere, velocity growth becomes more pronounced.

This progression highlights the interplay between forces acting on the rocket during its ascent, illustrating how it transitions from battling drag and gravity in the dense atmosphere to accelerating efficiently in thinner air.

By analyzing these parameters throughout the launch, engineers can fine-tune the rocket's flight path, ensuring a smooth ascent and a flawless transition into its intended parking orbit in low Earth orbit (LEO). which will serve as an intermediate stage before the final transfer to the Moon's orbit.

2.2 Orbital Mechanics

A successful lunar landing mission hinges on both a stable and well-designed rocket and a deep understanding of orbital mechanics. With the spacecraft on its way to its parking orbit, we can now begin analyzing the necessary orbital maneuvers that guide the spacecraft on its journey to the lunar celestial body. Orbital mechanics, the science governing object motion in space, provides the tools to calculate these trajectories. Concepts such as orbital elements, Kepler's laws of motion, orbital insertion, escape velocity, and orbital transfers become crucial in determining the maneuvers required for the spacecraft to escape Earth's gravity, reach the Moon's vicinity, and ultimately land safely on its surface.

2.2.1. Orbital Elements

An orbit is "an imaginary path followed by an object while it is moving under the influence of any other object". As shown in Figure 8, key parts and attributes of an orbit include:

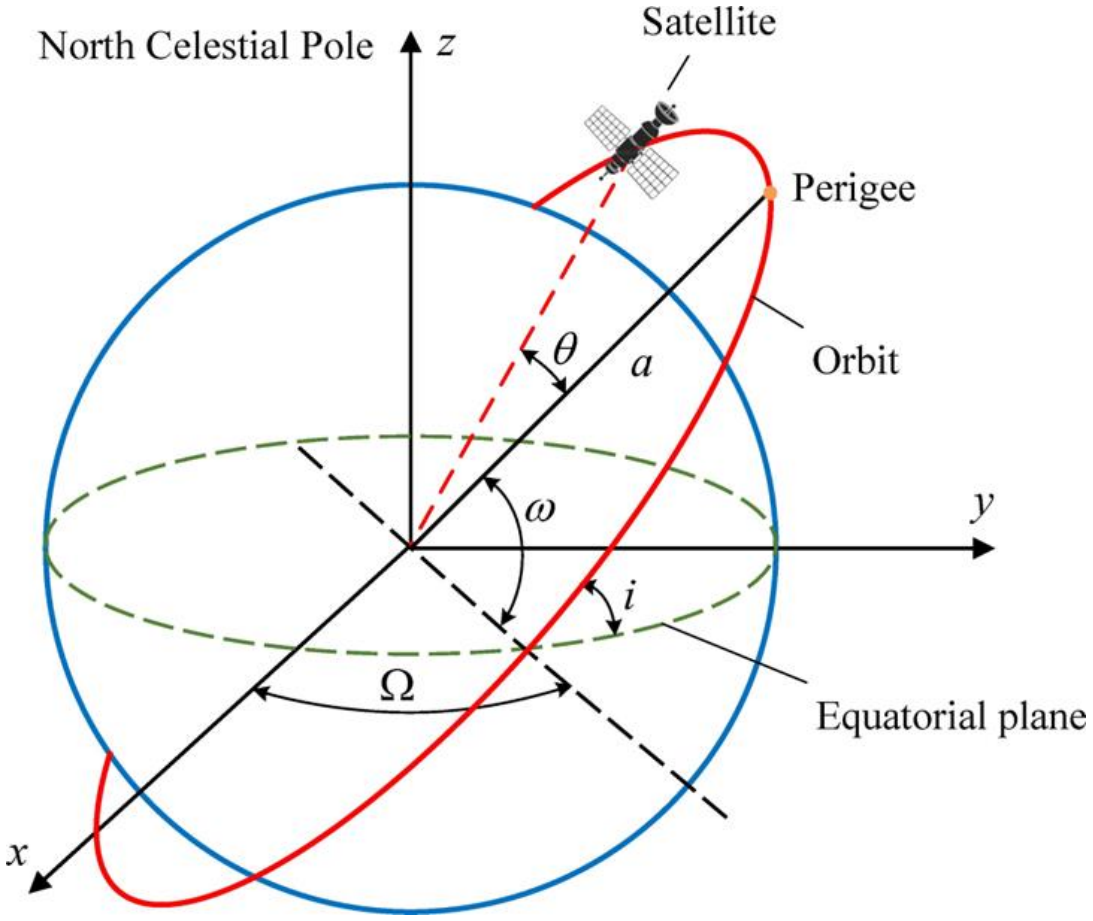

Figure-8 Orbital Elements (Luo, Q., Peng, W., Wu, G., Xiao, Y., 2022)

- **Semi-Major Axis (a):** The semi-major axis is the longest radius of an elliptical orbit, extending from the center of the ellipse to the farthest point on the orbit. For a circular orbit, the semi-major axis is simply the radius.
- **Eccentricity (e):** The eccentricity describes the shape of the orbit, specifically how elongated or "stretched out" it is. An orbit with e = 0 is perfectly circular, while an orbit with 0 < e < 1 is elliptical, and e = 1 is parabolic.

- **Periapsis and Apoapsis:**

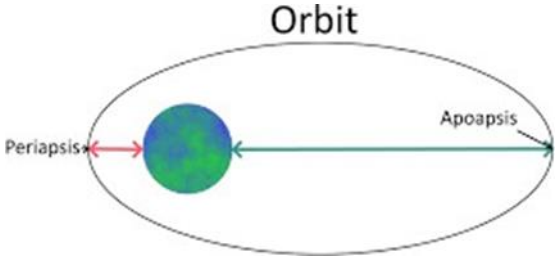

Figure-9 Periapsis vs. Apoapsis (Vij, 2022)

  - **Periapsis (or Perigee for Earth orbits):** Per Figure 9, the point of periapsis is the closest point of the orbit to the central body.
  - **Apoapsis (or Apogee for Earth orbits):** As shown in Figure 9, the apoapsis is the farthest point from the central body.
- **Inclination (i):** The inclination is the angle between the orbital plane and the equatorial plane of the central body (for example, Earth's equator).
- **Longitude of Ascending Node (Ω):** The longitude of the ascending node is the angle between a reference direction (such as the vernal equinox) and the ascending node, which is the point where the orbit crosses the equatorial plane from south to north.
- **Argument of Periapsis (ω):** The argument of periapsis defines the orientation of the ellipse within the orbital plane. It measures the angle between the ascending node and the point of periapsis.
- **True Anomaly (ν):** The true anomaly is the angle between the periapsis and the current position of the orbiting body, measured at the central body

Orbits vary in size and shape and can be elliptical, parabolic, or circular. For our mission, we will focus on circular orbits. With certain orbital elements, such as eccentricity, periapsis/apoapsis, and the argument of periapsis are less applicable to circular orbits as the object maintains a constant distance from the central body.

Additionally, orbits can be either bounded or unbounded. Bounded orbits, like circular and elliptical orbits, are closed paths that repeat. Unbounded orbits, such as parabolic and hyperbolic orbits, are open paths that do not repeat.

2.2.2. Johannes Kepler's Laws of Planetary Motion

With the fundamentals of orbits established, we can redirect our attention to Kepler's laws. Kepler's three laws of planetary motion describe how objects move in orbit, based on careful observations of the planets around the Sun. As depicted in the following figure, these laws provide fundamental insights into orbital mechanics and are essential for understanding the behavior of orbiting bodies.

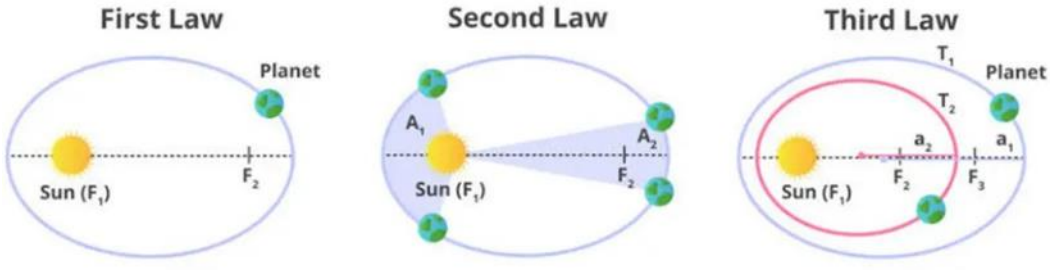

Figure-10 Kepler's Law of Planetary Motion (Soumyadeep, 2024)

1. **Kepler's First Law (Law of Ellipses):** All planets or satellites move in elliptical orbits with the Sun (or the central body) at one of the two foci.
2. **Kepler's Second Law (Law of Equal Areas):** A line connecting a planet (or satellite) to the Sun (or the central body) sweeps out equal areas at equal times. This law is reflected in the changing orbital speed

of the object. The body moves fastest at periapsis (A1) and slowest at apoapsis (A2). This variation in speed is directly linked to the semi-major axis of the orbit and the total orbital energy.

3. **Kepler's Third Law (Law of Harmonies):** The square of the orbital period (T) of a planet is directly proportional to the cube of the semi-major axis (a) of its orbit (T2 ∝ a3) which means that if the size of an orbit (through the semi-major axis) is known, you can determine the orbital period. The larger the orbit (greater a), the longer the period.

3.2.3. Orbital Insertion

Using our newfound knowledge of orbital elements and Kepler's Laws, we can now discuss the critical process of orbital insertion. Orbital insertion is the process of placing a spacecraft into a specific orbit around a celestial body. To achieve this, the spacecraft must:

1. **Attain the necessary orbital velocity:** This requires a significant acceleration imparted by the rocket engines. Orbital velocity dictates the speed at which the spacecraft orbits its parent body (Earth). Maintaining this precise velocity is crucial for a stable orbit.

For elliptical orbits, the orbital velocity varies at different points in the orbit. It is highest at periapsis and lowest at apoapsis. However, in the case of circular orbits, orbital velocity is equal to

$$v = \sqrt{(GM/r)} \tag{13}$$

where:

- $\boldsymbol{v}$ is the orbital velocity
- $\boldsymbol{G}$ is the universal gravitational constant/ centrifugal force (approximately 6.674 × 10-11 N m²/kg²)
- $\boldsymbol{M}$ is the mass of the central body (e.g., Earth)
- $\boldsymbol{r}$ is the radius of the orbit (distance from the center of the central body) depending on the mass of the central body and the radius of the orbit.

This equation shows that the orbital velocity depends on the mass of the central body and the radius of the orbit. A larger central body or a smaller orbital radius will result in a higher orbital velocity.

2. **Achieve the desired altitude:** This is accomplished through the continuous burning of the rocket's engines, propelling it upwards through the atmosphere.
3. **Establish the correct orbital inclination:** The rocket's trajectory must be carefully controlled to achieve the desired inclination of the orbit relative to the Earth's equator.
4. **Execute the orbital insertion burn:** At the apogee of the ascent trajectory, the spacecraft's engines are fired for a precise duration, providing the final velocity increment needed to achieve the desired circular orbit.

The orbital insertion process typically culminates in the establishment of a parking orbit, which allows for precise timing and alignment of subsequent burns, optimizing efficiency and increasing the likelihood of mission success.

2.2.4. Escape Velocity

Given the spacecraft is in its parking orbit, we can now apply the fundamental concepts of orbital mechanics to guide its transition from the inner parking orbit to its target orbit. To initiate this transition, it is essential to understand the velocity requirements for escaping or transferring between orbits.

Escape velocity is the minimum speed needed for an object to escape the gravitational pull of a massive body. If an object reaches an escape velocity, it can overcome the gravitational force and move indefinitely away from the body1. The formula for escape velocity is

$$v_{escape} = \sqrt{(2GM/r)} \tag{14}$$

where:

- $\boldsymbol{v_{escape}}$ is the escape velocity
- $\boldsymbol{G}$ is the universal gravitational constant

- ***M*** is the mass of the celestial body
- ***r*** is the distance from the center of the celestial body

For Earth, the escape velocity is approximately 11.2 km/s (11200 m/s). This means that a spacecraft must reach this speed to break free from Earth's gravitational pull and travel into deep space. Escape velocity depends on the spacecraft's altitude: The higher the parking orbit, the lower the escape velocity, because Earth's gravitational influence weakens with distance.

2.2.5. Orbital Transfers

With the vehicle meeting its escape velocity, we can begin the orbital transfer—a crucial process for moving a spacecraft from one orbit to another, typically around the same central body. Orbital transfers involve controlled changes in the spacecraft's velocity to adjust its orbital energy and trajectory, enabling the transition between orbits. The efficiency of a transfer is closely tied to delta-v, to minimize fuel consumption while achieving mission goals.

Efficient transfers require precise timing and alignment with the target orbit, as these factors ensure the maneuver's success and fuel economy. While various techniques such as bi-elliptic and low-thrust transfers exist, in this scenario—where the spacecraft transitions between two circular orbits—a Hohmann transfer is the most appropriate and commonly used method1. This maneuver, discussed in the following section, exemplifies how orbital mechanics and fuel optimization come together to achieve mission objectives.

2.2.5.1. Hohmann Transfer

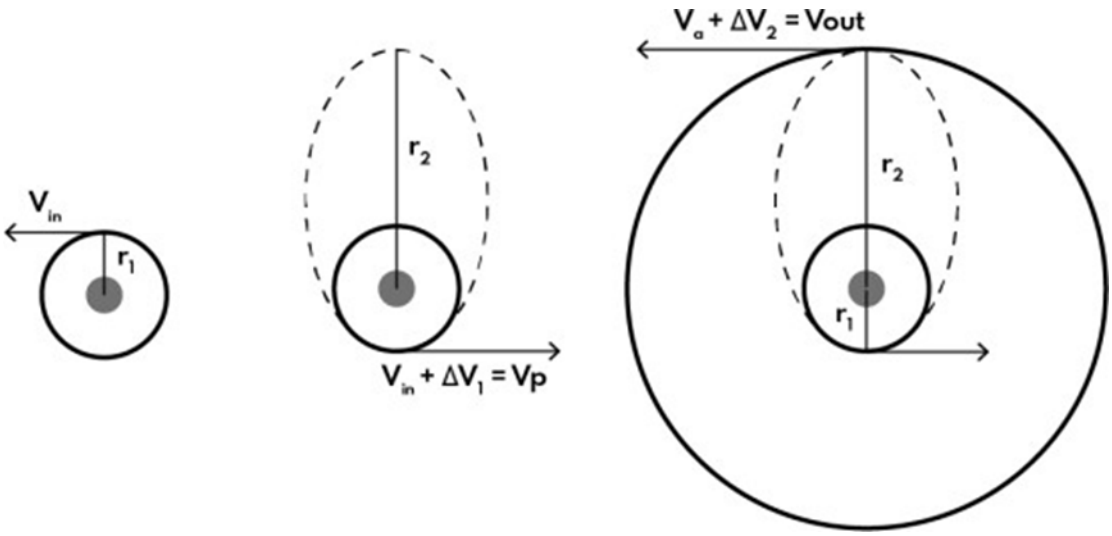

Figure-1 Hohmann Transfer Orbit (Space Technology and Aeronautical Rocketry, n.d.)

The Hohmann transfer, as shown in Figure 11, is a widely used transfer maneuver used to transfer spacecraft from LEO to the Moon, Mars, and asteroids (Space Technology and Aeronautical Rocketry, n.d.). The Hohmann transfer calculates the delta-v needed for orbital changes when it comes to moving from one circular orbit to another. It consists of two burns to provide the required velocities and consists of the following steps:

- **First orbital burn:** A burn is performed at the perigee of the initial circular, parking orbit to raise the spacecraft's apogee, transforming the circular orbit into an elliptical one.
- **Second orbital burn:** At the apogee of the newly formed elliptical orbit, a second burn is performed to circularize the orbit at the desired altitude, such as a lunar transfer orbit.

This sequence of burns allows the spacecraft to efficiently transfer from its initial parking orbit to the desired target orbit.

2.2.6. Exercise 2a: Calculating Orbital Parameters

Expanding on the success of a fully optimized and stable vehicle that has reached its trajectory, this exercise focuses on the precise calculations required for orbital maneuvers. Using Earth's parameters, such as its

gravitational constant (6.6743E-11Nm2/kg2) and radius (6378000 m), along with the target altitudes for inner and outer orbits, we will determine the orbital velocities required at each stage and the parameters of the transfer orbit. These calculations are essential for planning the trajectory from an initial circular orbit to a higher circular orbit, requiring a detailed understanding of orbital mechanics and the principles governing orbital transfers.

In this exercise, we will use established formulae and techniques to:

- Calculate the velocities for the inner and outer circular orbits based on their respective altitudes.
- Derive the characteristics of the transfer orbit, including its semi-major axis, eccentricity, and the velocity changes required at the points of departure and arrival.
- Evaluate how Earth's gravitational parameters influence the transfer trajectory and ensure a smooth transition between orbits.

By mastering these calculations, we gain the tools necessary to design efficient orbital maneuvers for missions involving satellite deployment, interplanetary transfers, or rendezvous operations.

Consider the following example: The spacecraft LEO at 400,000 m above the Earth's surface and needs to be transferred to a target orbit at 36,000,000 m:

Earth		
Parameters	Value	Unit
G	6.6743E-11	Nm2/kg2
Mass	5.9722E+24	kg
Radius	6378000	m
Gravitational Acceleration	9.81	m/s2
Inner Orbit		
Altitude	400000	m
Radius	6778000	m
Vin	7668.6559	m/s
Outer Orbit		
Altitude	36000000	m
Radius	42378000	m
Vout	3066.90134	m/s
	che	
Transfer Orbit		
Perigee	6778000	m
Apogee	42378000	m
Vp	10069.6925	m/s
Va	1610.56152	m/s
Delta-Vp	2401.03662	m/s
Delta-Va	1456.33982	m/s
a transfer	24578000	m

Figure-12 Calculating Orbital Parameters

Calculate Inner Orbit Parameters:

1. **Define the Altitude:** The height of the spacecraft's orbit above the Earth's surface (400,000 m).
2. **Calculate the Orbital Radius (r_{in}):** Add the Earth's radius to the altitude:

$$r_{in} = R + altitude \tag{15}$$

3. **Determine the Velocity (v_{in}):** Use the orbital velocity formula to calculate the velocity required to maintain a stable inner orbit:

$$V_{in} = \sqrt{G \cdot M \cdot (2/r_{in} - 1/r_{in})} \tag{16}$$

Calculate Outer Orbit Parameters:

1. **Define the Outer Orbit Altitude:** Choose the desired altitude for the outer orbit (36,000,000 m).
2. **Calculate the Outer Orbit Radius (r_{out}):** Add the inner orbit radius to the outer orbit altitude:

$$r_{out} = r_{in} + outer\ orbit\ altitude \tag{17}$$

3. **Determine the Outer Orbit Velocity (v_{out}):** Use the orbital velocity formula to calculate the velocity required to maintain the outer orbit:

$$v_{out} = \sqrt{G \cdot M \cdot (2/r_{out} - 1/r_{out})} \tag{18}$$

Calculate Transfer Orbit Parameters (Hohmann Transfer):

1. **Define Perigee and Apogee:**
   - **Perigee:** Closest point in the transfer orbit, equal to the radius of the inner orbit.
   - **Apogee:** Farthest point in the transfer orbit, equal to the radius of the outer orbit.
2. **Calculate the Transfer Orbit Radius ($r_{transfter}$): Find the average of the perigee and apogee distances:**

$$r_{transfter} = (r_{perigee} + r_{apogee})/2 \tag{19}$$

3. **Determine Velocity at Perigee (v_p): Use the transfer orbit velocity formula to find the spacecraft's velocity at perigee:**

$$V_p = \sqrt{G \cdot M \cdot (2/r_{perigee} - 1/r_{transfter})} \tag{20}$$

4. **Determine Velocity at Apogee (v_a): Similarly, calculate the spacecraft's velocity at apogee:**

$$V_a = \sqrt{G \cdot M \cdot (2/r_{apogee} - 1/r_{transfter})} \tag{21}$$

5. **Calculate Delta-v Requirements:**
   - **Delta-v at Perigee:** The change in velocity required to enter the transfer orbit.
   - **Delta-v at Apogee:** The change in velocity required transition into the outer orbit.

This step-by-step approach provides clear insights into orbital dynamics, emphasizing the relationships between gravitational forces, orbital velocities, and delta-v requirements.

By calculating each parameter, this exercise demonstrates the critical steps involved in planning orbital maneuvers and reinforces the practical application of orbital mechanics in mission planning.

2.2.7. Exercise 2b: Calculating Spacecraft Parameters

Spacecraft Parameters	
Thrust	40000
Isp	300
Mf	1200
Mo	2714.06
Mp	1514.06
Burn time	111.3969645

Figure-13 Calculating Spacecraft Parameters

Given the required delta-v for the perigee burn (2401.03 m/s) calculated in the previous section, a specific impulse (Isp) of 300 seconds, and a final spacecraft mass of 1200 kg, we can use the rocket equation to determine the initial mass (m0), the propellant mass (mp), and the burn time needed for the first burn.

1. **Rearrange the Rocket Equation (Equation (2)) to Find Initial mass (m0):**

$$m_0 = m_f \cdot exp(\Delta v/v_e)$$

2. **Calculate the Propellant Mass (mp):** The propellant mass is the difference between the initial mass and the final mass:

$$m_p = m_0 - m_f \tag{22}$$

3. **Determine the Burn Time:**

To calculate the burn time, we first determine the mass flow rate using the thrust and exhaust velocity

$$(Mass\ Flow\ Rate = Thrust/v_e) \tag{23}$$

Now, the burn time can be found by dividing the propellant mass by the mass flow rate

$$(Burn\ Time = m_p/Mass\ Flow\ Rate) \tag{24}$$

By performing similar calculations for the apogee burn, we can determine the total propellant mass required for the entire Hohmann transfer maneuver. This analysis allows us to assess the feasibility of the mission and optimize the spacecraft's design and trajectory.

3. Mission Design and Methodology

With the fundamentals of spaceflight established, we can now begin to plan our lunar lander mission. Our goal is to launch a 1000 kg payload to the Moon using a two-stage vehicle. This mission can be broken down into three primary phases:

1. **Sky is Not the Limit:** This phase focuses on launching the spacecraft from Earth and ascending beyond its atmosphere. The rocket's engines must generate sufficient thrust to overcome Earth's gravity and propel the spacecraft into space. To analyze this process, we will use Excel simulations to model the rocket's ascent, accounting for factors such as mass reduction, thrust, aerodynamic drag, and gravitational forces.
2. **To the Moon and Never Back:** Once the spacecraft has escaped Earth's gravity, it will be inserted into a parking orbit 300 km above Earth. Subsequent maneuvers, such as a Hohmann transfer, will propel the spacecraft toward the Moon. We will employ tools like GMAT to simulate these orbital maneuvers and calculate the required delta-v.
3. **A Giant Leap:** Upon reaching the Moon, the spacecraft will perform a series of maneuvers to slow down and achieve a soft landing on the lunar surface.

By carefully planning and executing these phases, and leveraging tools like Excel and GMAT, we can successfully deliver our payload to the Moon.

3.1. Phase 1: Sky is Not the Limit

The initial phase focuses on evaluating the launch vehicle's capabilities and the performance of its propulsion systems in propelling the spacecraft beyond Earth's atmosphere. This stage incorporates design strategies to optimize the launch trajectory and minimize fuel consumption, ensuring efficient and effective ascent.

3.1.2. Objectives

- Design a launch trajectory that safely propels the spacecraft beyond Earth's atmosphere and establishes a stable LEO.
- Determine the required delta-v (change in velocity) for this maneuver, considering the interplay between the spacecraft's thrust, gravitational pull (weight), and atmospheric drag.
- Optimize the burn profile to minimize fuel consumption while ensuring mission success.

3.1.3. Calculations and Simulations

First Stage	
Parameters	**Value**
Wet Mass	420000
Dry Mass	30000
Propellant Mass	390000
Diameter	3
Area	7.071428571
Cd	0.45
Isp	300
Thrust	9564750
Burn Time	120
Mass Flow Rate	3250

Second Stage	
Parameters	**Value**
Dry Mass	4000
Propellant Mass	92000
Wet Mass	96000

Parameters	Value
First stage	420000
Second stage	96000
Payload	1000
Total Mass	517000
Mass at the end of 1st burn out	127000

Atmospheric Conditions	
Parameters	**Value**
Density	1.22
Gravitational Acceleration	9.81

Figure-14 Phase 1: Calculating Launch Vehicle Parameters

t	vo	h	mf	mg	D	a	dv	Vf
0.1	0	0	517000	5071770	0	8.690483559	0.8690483559	0.869048
1	0.8690483559	0.3910717602	514075	5043075.75	1.466011551	8.795745337	7.916170803	8.785219
2	8.785219159	9.654267515	510825	5011193.25	149.8147962	8.913829463	8.913829463	17.69904
3	17.69904862	26.48426778	507575	4979310.75	608.0640844	9.032815221	9.032815221	26.73186
4	26.73186384	44.43091246	504325	4947428.25	1387.100692	9.152698457	9.152698457	35.88456
5	35.8845623	62.61642614	501075	4915545.75	2499.567184	9.273471402	9.273471402	45.15803
6	45.1580337	81.042596	497825	4883663.25	3958.398874	9.395125498	9.395125498	54.55315
7	54.5531592	99.7111929	494575	4851780.75	5776.826436	9.517651364	9.517651364	64.07081
8	64.07081056	118.6239698	491325	4819898.25	7968.378304	9.641038766	9.641038766	73.71184
9	73.71184933	137.7826599	488075	4788015.75	10546.88285	9.765276581	9.765276581	83.47712
10	83.47712591	157.1889752	484825	4756133.25	13526.47032	9.890352766	9.890352766	93.36747
11	93.36747868	176.8446046	481575	4724250.75	16921.57449	10.01625432	10.01625432	103.3837
12	103.383733	196.7512117	478325	4692368.25	20746.93408	10.14296726	10.14296726	113.5267
13	113.5267003	216.9104333	475075	4660485.75	25017.59385	10.27047657	10.27047657	123.7971
14	123.7971768	237.3238771	471825	4628603.25	29748.90531	10.39876616	10.39876616	134.1959
15	134.195943	257.9931198	468575	4596720.75	34956.5272	10.52781886	10.52781886	144.7237
16	144.7237619	278.9197048	465325	4564838.25	40656.42553	10.65761634	10.65761634	155.3813
17	155.3813782	300.1051401	462075	4532955.75	46864.87318	10.7881391	10.7881391	166.1695
18	166.1695173	321.5508955	458825	4501073.25	53598.44922	10.91936643	10.91936643	177.0888
19	177.0888837	343.258401	455575	4469190.75	60874.03764	11.05127633	11.05127633	188.1401
20	188.1401601	365.2290438	452325	4437308.25	68708.82569	11.18384552	11.18384552	199.3240
21	199.3240056	387.4641656	449075	4405425.75	77120.3017	11.31704938	11.31704938	210.6410
22	210.6410549	409.9650605	445825	4373543.25	86126.25236	11.45086188	11.45086188	222.0919
23	222.0919168	432.7329718	442575	4341660.75	95744.75949	11.58525558	11.58525558	233.6771
24	233.6771724	455.7690892	439325	4309778.25	105994.1961	11.72020157	11.72020157	245.3973

Figure-15 Phase 1: Trajectory Simulation

24	233.6771724	455.7690892	439325	4309778.25	105994.1961	11.72020157	11.72020157	245.3973
25	245.397374	479.0745464	436075	4277895.75	116893.222	11.85566939	11.85566939	257.2530
26	257.2530434	502.6504174	432825	4246013.25	128460.7787	11.99162703	11.99162703	269.2446
27	269.2446704	526.4977138	429575	4214130.75	140716.0833	12.12804089	12.12804089	281.3727
28	281.3727113	550.6173817	426325	4182248.25	153678.6223	12.26487569	12.26487569	293.6375
29	293.637587	575.0102983	423075	4150365.75	167368.1442	12.40209444	12.40209444	306.0396
30	306.0396814	599.6772684	419825	4118483.25	181804.6513	12.53965843	12.53965843	318.5793
31	318.5793399	624.6190213	416575	4086600.75	197008.3908	12.67752712	12.67752712	331.2568
32	331.256867	649.8362068	413325	4054718.25	212999.8451	12.81565815	12.81565815	344.0725
33	344.0725251	675.3293921	410075	4022835.75	229799.721	12.95400726	12.95400726	357.0265
34	357.0265324	701.0990575	406825	3990953.25	247428.9382	13.09252827	13.09252827	370.1190
35	370.1190607	727.145593	403575	3959070.75	265908.6164	13.23117298	13.23117298	383.3502
36	383.3502336	753.4692943	400325	3927188.25	285260.062	13.36989118	13.36989118	396.7201
37	396.7201248	780.0703584	397075	3895305.75	305504.7531	13.5086306	13.5086306	410.2287
38	410.2287554	806.9488802	393825	3863423.25	326664.3241	13.64733683	13.64733683	423.8760
39	423.8760922	834.1048477	390575	3831540.75	348760.5481	13.78595328	13.78595328	437.6620
40	437.6620455	861.5381378	387325	3799658.25	371815.3193	13.92442117	13.92442117	451.5864
41	451.5864667	889.2485122	384075	3767775.75	395850.6336	14.06267947	14.06267947	465.6491
42	465.6491462	917.2356129	380825	3735893.25	420888.5678	14.20066483	14.20066483	479.8498
43	479.849811	945.4989571	377575	3704010.75	446951.2578	14.33831157	14.33831157	494.1881
44	494.1881226	974.0379335	374325	3672128.25	474060.8755	14.47555166	14.47555166	508.6636
45	508.6636742	1002.851797	371075	3640245.75	502239.6037	14.61231462	14.61231462	523.2759
46	523.2759888	1031.939663	367825	3608363.25	531509.6107	14.74852753	14.74852753	538.0245
47	538.0245164	1061.300505	364575	3576480.75	561893.0227	14.884115	14.884115	552.9086
48	552.9086314	1090.933148	361325	3544598.25	593411.8944	15.01899912	15.01899912	567.9276
49	567.9276305	1120.836262	358075	3512715.75	626088.1792	15.15309941	15.15309941	583.0807
50	583.0807299	1151.00836	354825	3480833.25	659943.6968	15.28633285	15.28633285	598.3670
51	598.3670627	1181.447793	351575	3448950.75	695000.1	15.41861381	15.41861381	613.7856
52	613.7856766	1212.152739	348325	3417068.25	731278.8392	15.54985405	15.54985405	629.3355
53	629.3355306	1243.121207	345075	3385185.75	768801.1261	15.67996269	15.67996269	645.0154

Figure-16 Phase 1: Trajectory Simulation (2)

52	613.7856766	1212.152739	348325	3417068.25	731278.8392	15.54985405	15.54985405	629.3355
53	629.3355306	1243.121207	345075	3385185.75	768801.1261	15.67996269	15.67996269	645.0154
54	645.0154933	1274.351024	341825	3353303.25	807587.8952	15.80884621	15.80884621	660.8243
55	660.8243395	1305.839833	338575	3321420.75	847659.7638	15.93640844	15.93640844	676.7607
56	676.7607479	1337.585087	335325	3289538.25	889036.9904	16.06255054	16.06255054	692.8232
57	692.8232985	1369.584046	332075	3257655.75	931739.4316	16.18717103	16.18717103	709.0104
58	709.0104695	1401.833768	328825	3225773.25	975786.4971	16.31016575	16.31016575	725.3206
59	725.3206352	1434.331105	325575	3193890.75	1021197.103	16.43142793	16.43142793	741.7520
60	741.7520632	1467.072698	322325	3162008.25	1067989.625	16.55084814	16.55084814	758.3029
61	758.3029113	1500.054974	319075	3130125.75	1116181.845	16.66831436	16.66831436	774.9712
62	774.9712257	1533.274137	315825	3098243.25	1165790.905	16.78371201	16.78371201	791.7549
63	791.7549377	1566.726163	312575	3066360.75	1216833.251	16.89692394	16.89692394	808.6518
64	808.6518616	1600.406799	309325	3034478.25	1269324.577	17.00783051	17.00783051	825.6596
65	825.6596921	1634.311554	306075	3002595.75	1323279.773	17.11630965	17.11630965	842.7760
66	842.7760018	1668.435694	302825	2970713.25	1378712.867	17.22223688	17.22223688	859.9982
67	859.9982387	1702.77424	299575	2938830.75	1435636.962	17.3254854	17.3254854	877.3237
68	877.323724	1737.321963	296325	2906948.25	1494064.183	17.42592615	17.42592615	894.7496
69	894.7496502	1772.073374	293075	2875065.75	1554005.61	17.52342793	17.52342793	912.2730
70	912.2730781	1807.022728	289825	2843183.25	1615471.219	17.61785743	17.61785743	929.8909
71	929.8909356	1842.164014	286575	2811300.75	1678469.818	17.70907941	17.70907941	947.6000
72	947.600015	1877.490951	283325	2779418.25	1743008.984	17.79695673	17.79695673	965.3969
73	965.3969717	1912.996987	280075	2747535.75	1809094.995	17.88135055	17.88135055	983.2783
74	983.2783223	1948.675294	276825	2715653.25	1876732.768	17.96212041	17.96212041	1001.240
75	1001.240443	1984.518765	273575	2683770.75	1945925.794	18.03912439	18.03912439	1019.279
76	1019.279567	2020.52001	270325	2651888.25	2016676.066	18.11221931	18.11221931	1037.391
77	1037.391786	2056.671353	267075	2620005.75	2088984.021	18.1812608	18.1812608	1055.573
78	1055.573047	2092.964834	263825	2588123.25	2162848.465	18.24610361	18.24610361	1073.819
79	1073.819151	2129.392198	260575	2556240.75	2238266.516	18.30660169	18.30660169	1092.125
80	1092.125752	2165.944903	257325	2524358.25	2315233.531	18.36260845	18.36260845	1110.488
81	1110.488361	2202.614113	254075	2492475.75	2393743.047	18.41397699	18.41397699	1128.902

Figure-17 Phase 1: Trajectory Simulation (3)

80	1092.125752	2165.944903	257325	2524358.25	2315233.531	18.36260845	18.36260845	1110.488
81	1110.488361	2202.614113	254075	2492475.75	2393743.047	18.41397699	18.41397699	1128.902
82	1128.902338	2239.390699	250825	2460593.25	2473786.713	18.4605603	18.4605603	1147.362
83	1147.362898	2276.265236	247575	2428710.75	2555354.232	18.50221152	18.50221152	1165.865
84	1165.86511	2313.228008	244325	2396828.25	2638433.295	18.53878422	18.53878422	1184.403
85	1184.403894	2350.269004	241075	2364945.75	2723009.527	18.57013263	18.57013263	1202.974
86	1202.974027	2387.377921	237825	2333063.25	2809066.425	18.59611195	18.59611195	1221.570
87	1221.570139	2424.544165	234575	2301180.75	2896585.306	18.61657868	18.61657868	1240.186
88	1240.186717	2461.756856	231325	2269298.25	2985545.257	18.63139087	18.63139087	1258.818
89	1258.818108	2499.004825	228075	2237415.75	3075923.081	18.6404085	18.6404085	1277.458
90	1277.458517	2536.276625	224825	2205533.25	3167693.254	18.64349381	18.64349381	1296.102
91	1296.10201	2573.560527	221575	2173650.75	3260827.885	18.64051163	18.64051163	1314.742
92	1314.742522	2610.844532	218325	2141768.25	3355296.674	18.63132979	18.63132979	1333.373
93	1333.373852	2648.116374	215075	2109885.75	3451066.881	18.61581945	18.61581945	1351.989
94	1351.989671	2685.363523	211825	2078003.25	3548103.298	18.59385555	18.59385555	1370.583
95	1370.583527	2722.573198	208575	2046120.75	3646368.223	18.56531716	18.56531716	1389.148
96	1389.148844	2759.732371	205325	2014238.25	3745821.443	18.53008795	18.53008795	1407.678
97	1407.678932	2796.827776	202075	1982355.75	3846420.222	18.48805655	18.48805655	1426.166
98	1426.166988	2833.84592	198825	1950473.25	3948119.297	18.43911708	18.43911708	1444.606
99	1444.606106	2870.773094	195575	1918590.75	4050870.874	18.3831695	18.3831695	1462.989
100	1462.989275	2907.595381	192325	1886708.25	4154624.64	18.32012016	18.32012016	1481.309
101	1481.309395	2944.29867	189075	1854825.75	4259327.776	18.24988218	18.24988218	1499.559
102	1499.559277	2980.868673	185825	1822943.25	4364924.979	18.172376	18.172376	1517.731
103	1517.731653	3017.290931	182575	1791060.75	4471358.495	18.08752981	18.08752981	1535.819
104	1535.819183	3053.550837	179325	1759178.25	4578568.156	17.99528004	17.99528004	1553.814
105	1553.814463	3089.633646	176075	1727295.75	4686491.428	17.8955719	17.8955719	1571.710
106	1571.710035	3125.524498	172825	1695413.25	4795063.468	17.7883598	17.7883598	1589.498
107	1589.498395	3161.20843	169575	1663530.75	4904217.188	17.67360791	17.67360791	1607.172
108	1607.172003	3196.670398	166325	1631648.25	5013883.335	17.55129064	17.55129064	1624.723
109	1624.723294	3231.895296	163075	1599765.75	5123990.568	17.42139312	17.42139312	1642.144
110	1642.144687	3266.86798	159825	1567883.25	5234465.558	17.28391173	17.28391173	1659.428
111	1659.428598	3301.573285	156575	1536000.75	5345233.093	17.13885459	17.13885459	1676.567
112	1676.567453	3335.996051	153325	1504118.25	5456216.187	16.98624205	16.98624205	1693.553
113	1693.553695	3370.121148	150075	1472235.75	5567336.212	16.8261072	16.8261072	1710.379
114	1710.379802	3403.933497	146825	1440353.25	5678513.026	16.65849633	16.65849633	1727.038
115	1727.038299	3437.418101	143575	1408470.75	5789665.124	16.48346945	16.48346945	1743.521
116	1743.521768	3470.560066	140325	1376588.25	5900709.79	16.30110073	16.30110073	1759.822
117	1759.822869	3503.344637	137075	1344705.75	6011563.262	16.11147903	16.11147903	1775.934
118	1775.934348	3535.757216	133825	1312823.25	6122140.912	15.9147083	15.9147083	1791.849
119	1791.849056	3567.783404	130575	1280940.75	6232357.426	15.71090809	15.71090809	1807.559
120	1807.559964	3599.40902	127325	1249058.25	6342127.004	15.50021398	15.50021398	1823.060

Figure-18 Phase 1: Trajectory Simulation (4)

To simulate the launch of a multistage rocket, we began by empathizing with the challenges faced by aerospace engineers in designing and optimizing rocket trajectories. We understood the need to accurately model the complex interplay between forces, mass, and energy during the launch process.

Next, we defined the problem as a multi-stage simulation that would track the rocket's position, velocity, and acceleration over time. Key parameters, such as initial mass, thrust, specific impulse, and atmospheric conditions, were identified as crucial inputs to the simulation.

To ideate a solution, we adopted a numerical integration approach, using a time-stepping method to calculate the rocket's trajectory. We broke down the simulation into smaller time steps, updating the rocket's state variables at each step based on the forces acting upon it.

The prototype for this simulation was implemented in Excel. We developed a spreadsheet model that incorporated the following steps:

1. **Initial Conditions:** Defined the initial mass, thrust, specific impulse, and other relevant parameters.
2. **Time-Step Calculation:** Calculated the change in velocity and position at each time step based on the net force and acceleration.
3. **Mass Update:** Accounted for the reduction in mass due to propellant consumption.
4. **Atmospheric Drag:** Incorporated the effects of atmospheric drag on the rocket's motion.
5. **Gravitational Force:** Considered the varying gravitational force as the rocket ascends.

By refining our model, we were able to test and learn from the simulation results. We analyzed the impact of different parameters on the rocket's trajectory and identified potential areas for optimization.

This approach allowed us to develop a robust and accurate simulation tool that can be used to analyze various rocket designs and mission scenarios.

3.1.3.1. Formulae

- Rocket Equation (Equation (2))
- Newton's Second Law of Motion (Equation (1))
- Area of a Circular Cross-Section

$$(A = \pi d^2/4) \tag{25}$$

- Thrust

$$thrust = (I_{so} * m_p * g_0)/burntime \tag{26}$$

- Mass Flow Rate (Equation (23))
- Drag Force (Equation (8))
- Kinematic Equations (Equation (4), Equation (5))
- Staging Mass Relations (Equation (22)

3.2. Phase 2: Orbital Insertion & Trans-Lunar Injection (TLI)

Once Earth escape is achieved, the spacecraft needs to be inserted into a 300 km parking orbit. From the parking orbit, a series of three orbit-raising maneuvers can be conducted. These maneuvers, planned and simulated using GMAT software, incrementally increase the spacecraft's velocity to the required 10.8 km/s for Trans-Lunar Injection (TLI).TLI will then propel the spacecraft on a trajectory toward the Moon.

3.2.1. Objectives

Establish a stable circular parking orbit at a targeted altitude of 300 km around Earth.

- Perform any necessary orbital maneuvers to achieve the desired 300 km circular orbit, considering factors like residual launch vehicle velocity and orbital plane adjustments.
- Optimize the burn profile(s) for this maneuver to minimize propellant consumption while ensuring a safe and efficient orbital insertion.
- Conduct a series of three optimized orbit-raising maneuvers to reach the desired TLI apogee. Utilize mission analysis tools to verify trajectory corrections.
- Calculate the precise delta-v for TLI, considering the final orbit and desired lunar transfer trajectory. Evaluate burn window opportunities and develop a preliminary fuel-efficient burn profile targeting 10.8 km/s injection velocity.

3.2.2. Calculations and Simulations

Earth Parking Orbit	
Altitude	300000
Radius of Orbit	6678000
Velocity	7725.859858

Spacecraft Properties	
Dry Mass	1200
Total Fuel	2248.248588

Transfer Orbit	
Earth to Moon Distance	384400000
Perigee	6678000
Apogee	384400000
Semi-Major Axis	195539000
Vp	10832.32847
Va	188.1849363
Delta-V required	3106.46861

1st Maneuver	
Inputs	
Apogee	15000000
F	70000
Isp	300
Elliptical Orbit	
Vp	9088.617943
Va	4046.252708
Delta-Vp	1362.758085
Spacecraft	
Mo	3448.248588
Mf	2170.192317
Mp	1278.056271

2nd Maneuver	
Inputs	
Apogee	18000000
F	70000
Isp	300
Elliptical Orbit	
Vp	9331.32029
Va	3461.919828
Delta-Vp	242.7023468
Spacecraft	
Mo	2170.192317
Mf	1998.402519
Mp	171.7897978

TLI	
Inputs	
Apogee	384400000
F	70000
Isp	300
Elliptical Orbit	
Vp	10832.32847
Va	188.1849363
Delta-Vp	1501.008178
Spacecraft	
Mo	1998.402519
Mf	1200
Mp	798.4025189

Figure-19 Phase 2: Orbital Insertion and TLI Calculations

3.2.2.1. Parking Orbit

Figure-20 Phase 2: Parking Orbit (GMAT)

To initiate the lunar transfer, we first established a stable parking orbit at an altitude of 300 km. To achieve this, we empathized with the need to accurately calculate the required delta-v for the orbital insertion burn, considering factors like the initial orbital velocity and the desired altitude.

Defining the problem involved identifying the specific parameters of the parking orbit, such as its semi-major axis and eccentricity.

Ideating and prototyping the solution involved simulating the orbital insertion maneuver using GMAT as displayed in Figure 20.

3.2.2.2. Maneuvers 1 and 2

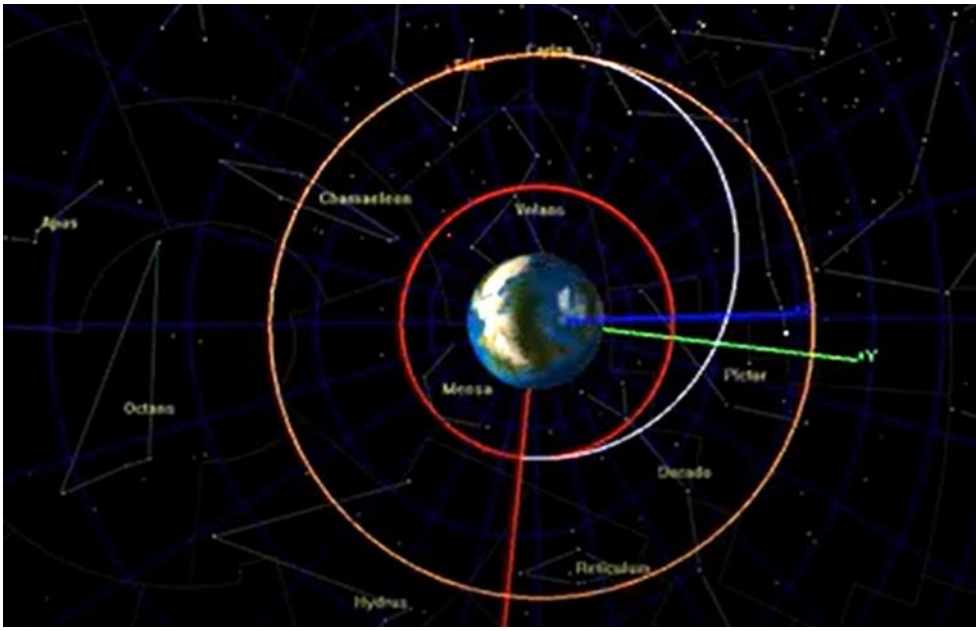

Figure-21 Phase 2: Orbital Maneuvers

After establishing the stable parking orbit at 300 km, we initiated a series of orbital maneuvers to position the spacecraft for lunar transfer. The first maneuver, as depicted in Figure 21, involved a precise burn to raise the apogee of the orbit from 300 km to 15,000 km. This significantly elongated the orbit, positioning the spacecraft for the next maneuver.

Subsequently, a second burn (not pictured) was executed to further raise the apogee to 18,000 km. This maneuver brought the spacecraft closer to the desired trajectory for lunar transfer, setting the stage for the final, critical burn.

To execute these maneuvers, we calculated the required delta-v, initial mass, propellant mass, and burn time for each burn. By carefully considering factors like engine performance, fuel efficiency, and orbital mechanics, we optimized the trajectory and ensured the spacecraft's successful transfer to the Moon.

3.2.2.3. Trans-Lunar Injection

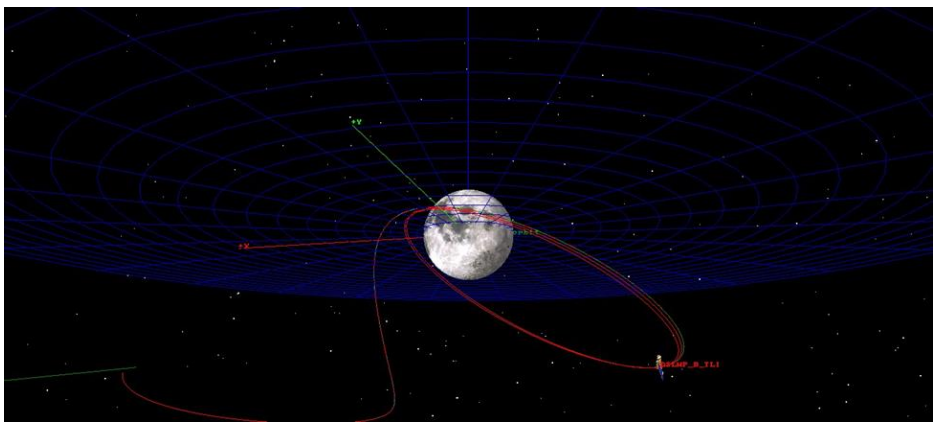

Figure-22 Phase 2: TLI (GMAT)

After the second burn in which the spacecraft achieved the raised orbit with an apogee of 18,000 km, the final task was to execute the TLI burn (Figure 22). This maneuver allowed the spacecraft with a velocity of 10.8 km/s to overcome Earth's gravitational pull and establish its trajectory toward the Moon. In planning this maneuver, we carefully accounted for the gravitational influences of both Earth and the Moon to ensure a precise and efficient transfer trajectory. Given the tight fuel constraints, there was very little room for error, making accurate calculations and execution critical to mission success.

3.2.2.4. Formulae

- Radius of Orbit (Equation (15))
- Velocity in orbit (Equation (16))
- Total Fuel (Equation (22))
- Radii of Perigee and Apogee
  - $r_{perigee} = r_{Earth\ partking\ orbit}$
  - $r_{apogee} = r_{Earth-Moon\ distance}$
- Semi-major axis

$$a = (r_{perigee} r_{orbit\ apogee})/2 \tag{27}$$

- Elliptical Orbit Velocities (Equation (20), Equation (21))
- Initial and Final Mass

$$m_0 = m_f * e^{\Delta v}/(I_{sp} * g_0) \tag{28}$$

- Burn Time

$$t_{burn} = (I_{sp} * g_0 * m_p)/T \tag{29}$$

3.3. Phase 3: A Giant Leap

The final and most delicate phase involves the powered descent and landing on the lunar surface. With the spacecraft positioned ~600m above the Lunar surface, design thinking is crucial in this phase for identifying opportunities, such as leveraging lunar gravity, and addressing hazards in the lunar environment to ensure a safe and controlled landing.

4.3.1. Objectives

- Design a controlled descent trajectory that safely guides the spacecraft from lunar orbit to a targeted landing site on the Moon's surface.
- Develop a powered descent burn profile that optimizes fuel consumption while ensuring proper engine throttling and deceleration for a soft lunar touchdown.
- Perform Science

4.3.2. Calculations and Simulations

Spacecraft Parameters	
Mo	1000

Free Fall Phase 1	
Input	
Initial H	600
Gravitational Acceleration	1.62
Final H	212.5

Propulsion Parameter	
Isp	330
Delta-V	54.8640548
M final	983.1783248
M fuel	16.8216752
M dot	1.402454154
F	4535.536733

Output	
Time	21.87224409
Velocity at the end of fall	35.43303543

Power Decent Values	
Initial V	35.43303543
Final V	0
Average V	17.71651772
Time	11.9944564

13	1000	1620	1.62	21.06	463.11
14	1000	1620	1.62	22.68	441.24
15	1000	1620	1.62	24.3	417.75
16	1000	1620	1.62	25.92	392.64
17	1000	1620	1.62	27.54	365.91
18	1000	1620	1.62	29.16	337.56
19	1000	1620	1.62	30.78	307.59
20	1000	1620	1.62	32.4	276
21	1000	1620	1.62	34.02	242.79
21.87224	1000	1620	1.62	35.43304	212.5

Figure-23 Phase 3: Spacecraft Parameters During Freefall

As exemplified in Figure 23, the lander initiates a controlled, free-fall descent from an altitude of 600 meters to a critical altitude of 212.5 meters above the lunar surface. By using our understanding of the spacecraft's propulsion parameters, lunar gravity, and the desired landing altitude, we can calculate the necessary free-fall time and velocity. This controlled descent minimizes fuel consumption while ensuring a safe and soft landing. Any deviation from the planned trajectory or unexpected events during the descent could result in the loss of the payload and compromise the mission's scientific objectives.

Landing Trajectory Parameters					
Time	Mf	Mg	a	v	H
0	1000	1620	1.62	35.43303543	212.5
1	998.5975458	1617.728024	-2.92191	32.51112888	178.5279
2	997.1950917	1615.456049	-2.92829	29.5828346	147.4809
3	995.7926375	1613.184073	-2.9347	26.6481346	119.3655
4	994.3901834	1610.912097	-2.94112	23.70701079	94.18788
5	992.9877292	1608.640121	-2.94757	20.75944505	71.95465
6	991.5852751	1606.368146	-2.95403	17.80541915	52.67222
7	990.1828209	1604.09617	-2.9605	14.84491479	36.34705
8	988.7803668	1601.824194	-2.967	11.87791358	22.98564
9	987.3779126	1599.552218	-2.97352	8.904397081	12.59448
10	985.9754585	1597.280243	-2.98005	5.924346751	5.18011
11	984.5730043	1595.008267	-2.9866	2.937743977	0.749065
12	983.1705502	1592.736291	-2.99317	-0.055429935	-0.69209

Figure-24 Phase 3: Landing Trajectory Parameters

When the lander reaches an altitude of 212.5 meters, the engines ignite for a final burn to slow the descent and ensure a soft landing. This phase, captured in Figure 24, depicts the final 12 seconds before touchdown. It is evident from the figure that the lander is decelerating as it approaches the lunar surface, as indicated by the decreasing altitude and velocity over time.

3.3.2.3. Deceleration/ Touchdown

Using high-precision timing and control of the lander's thrusters, the final phase of the descent aims to gradually reduce the lander's velocity to zero at the precise moment of touchdown.

3.3.2.4. Formulae

- Altitude

$$H = (½)gt^2 \tag{30}$$

- Velocity at end of fall

$$v = gt \tag{31}$$

- Average Velocity

$$V_{average} = V_{initial}/2 \tag{32}$$

- Time

$$t = (2H)/v \tag{33}$$

- Rocket Equation (Equation (2))
- Thrust (Equation (26))

4. Conclusion

During my internship, I applied design thinking principles to optimize a lunar lander mission. By leveraging my knowledge of rocket stability and orbital mechanics, I successfully navigated the design process, from empathizing with the mission's objectives to testing and refining the lunar landing strategy. I utilized Excel and GMAT to conduct a detailed simulation of the lander's mission, focusing on optimizing ascent, orbital maneuvers, and landing trajectories to minimize propellant expenditure. This practical experience solidified my understanding of aerospace engineering principles and the value of a user-centered approach to problem-solving

5. Acknowledgement

I would like to express my sincere gratitude to my mentors at Space Technology & Aeronautical Rocketry (STAR), located in Surat, Gujarat, India, for providing me with the research topic and invaluable guidance throughout my internship. Their expertise in aviation and aerospace component manufacturing, coupled with their commitment to innovation, enriched my learning experience.

6. Disclosures

During the preparation of this work, the author used ChatGPT to enhance clarity and fluency of expression. After using this tool/service, the author reviewed and edited the content as needed and takes full responsibility for the content of the publication.

7. References

[1] Ansys Innovation Courses. (n.d.). Oblique shock waves. Ansys. Retrieved from https://innovationspace.ansys.com/courses/courses/shock-expansion-theory/lessons/oblique-shock-waves-lesson-3/
[2] Byju's. (n.d.). Rocket propulsion. Retrieved from https://byjus.com/physics/rocket-propulsion/
[3] Finio, B. (2023, September 14). Model rocket aerodynamics: Stability. Science Buddies. Retrieved from https://www.sciencebuddies.org/science-fair-projects/project-ideas/Aero_p002/aerodynamics-hydrodynamics/model-rocket-stability
[4] Greer, M. (2020, February 24). Design thinking: An introduction. Usability Geek. Retrieved from https://usabilitygeek.com/start-here/
[5] Luo, Q., Peng, W., Wu, G., & Xiao, Y. (2022, April 19). Orbital maneuver optimization of Earth observation satellites using an adaptive differential evolution algorithm. Remote Sensing, 14(9), 1966. MDPI. Retrieved from https://www.mdpi.com/2072-4292/14/9/1966
[6] Microsoft Corporation. (2021). Microsoft Excel (Version 2021) [Computer software]. Retrieved from https://www.microsoft.com/en-us/microsoft-365/excel
[7] National Aeronautics and Space Administration. (2025). General Mission Analysis Tool (GMAT).
[8] OpenAI. (2023). ChatGPT (Mar 14 version) [Large language model]. Retrieved from https://chat.openai.com/chat
[9] Sawada, H., et al. (2014). Development of a lunar lander simulation software for educational purposes. Sensors, 14(9), 1966–1982.
[10] Soumyadeep. (2024, October 3). Kepler’s law of planetary motion for class 11: Get Kepler first and second laws. Adda247. Retrieved from https://www.adda247.com/school/keplers-laws-of-planetary-motion/
[11] Space Technology & Aeronautical Rocketry. (2023). Orbital mechanics guide (1st ed.).
[12] Vij, R. (2022, June 16). The Oberth effect: How does it work? [Blog post]. Medium. Retrieved from https://medium.com/@rohankvij/the-oberth-effect-how-does-it-work-astronautics-for-dummies-part-1-15ee1b20eb40

8. References

The author declares no competing conflict of interest.

9. Funding

No funding was issued for this research.